Journal of Chemical Health Risks

www.jchr.org

JCHR (2026) 16(2), 2743 - 2754

Synergistic Antioxidant Activity of Green-Synthesized Iron Oxide Nanoparticles: A Comparative Study of Capparis decidua Phytochemical-Mediated Synthesis and In Vitro Evaluation

Abdul Majeed Ansari[1] & Dinesh[2*]

[1]*Research Scholar, Department of Chemistry, Career Point University, Kota, Rajasthan, India-324005*
[2]*Assistant Professor, Department of Chemistry, Career Point University, Kota, Rajasthan, India-324005*

Received: 24 February 2026 *Accepted:17 March 2026* *Published: 06 April 2026*

KEYWORDS

Green synthesis, iron oxide nanoparticles, Capparis decidua, antioxidant activity, phytochemicals

ABSTRACT:

Oxidative stress is a primary etiological agent in most chronic illnesses, hence the necessities the development of effective antioxidant interventions. In this study, the antioxidant synergy between iron oxide nanoparticles (FeONPs) prepared by the use of a green chemistry method that utilizes aqueous extracts of Capparis decidedua was evaluated, a botanical source rich in polyphenolic compounds. The phyto-mediated reaction used ferric chloride hexahydrate as the metal ion precursor and the bioactives in the plants served as reducing and stabilizing agents. Full physicochemical characterization through ultraviolet-visible spectroscopy depicted typical surface plasmon resonance pinnacles at 242, 385, 422, and 477nm, thus establishing nanoparticle development. Fourier-transform infrared spectroscopy analysis indicates the presence of phytochemical adsorption onto the surfaces of the nanoparticles. The measurements of dynamic light scattering determined a hydrodynamic diameter of 88.5nm and a moderate colloidal stability (zeta potential = -28.3mV). Dose-dependent in vitro antioxidant assessment using DPPH, ABTS, and nitric oxide radical scavenging showed an IC50 of 47.82 ± 1.86, 64.31 ± 0.97, and 68.54 ± 0.79 µg/mL mg/ml, respectively. Notably, FeONPs also exhibited much greater antioxidant activity as compared to the plant extract itself, and this is indicative of synergy, which can be ascribed to the interplay between the phytochemical corona and the nanoparticle core. These findings support green-syntheses FeONPs as attractive options to be used as therapeutic agents in oxidative stress-linked diseases, which have advantages in the aspects of biocompatibility, multifunctional features, and sustainable synthesis.

1. Introduction

Oxidative stress, an unequivocal mismatch of reactive oxygen species (ROS) generation and antioxidant defense mechanism capacities, represents a fundamental pathophysiological marker of an array of chronic diseases, like cardiovascular diseases, neurodegenerative diseases, diabetes mellitus, and malignancies (Jomova et al., 2023). The accumulated ROS cause cell injury through lipid peroxidation, oxidation of proteins, and fragmentation of DNA and this impairs cellular homeostasis and organ functioning (Bartsch & Nair, 2006). The restoration of redox balance by the use of antioxidant supplements is a priority of modern therapeutic practices; nevertheless, conventional synthetic antioxidants have disadvantages, including low bioavailability, quick metabolic elimination, and potential cytotoxicity of clinically relevant concentrations (Al-Madhagi & Masoud, 2024). Medicinal plants are natural sources of phenolics, flavonoids, alkaloid, and terpenoid natural antioxidants, and they have the capacity to neutralize ROS by different mechanisms, such as hydrogen atom transfer, single-electron transfer, and metal chelation (Kovacic et al., 2015). One such botanical source is Capparis decidua, also known as karira or caper berry that is traditionally used in Ayurvedic and Unani medicine to treat inflammatory diseases, diabetes, and oxidative-associated conditions (Pal et al., 2021). This is a xerophytic shrub that has been found to be a good store of phytobiotic compounds, including quercetin, kaempferol, rutin, gallic acid, chlorogenic acid, stachydrine, and diverse glucosinolates, induced by phytochemical research (Ayan et al., 2025; Nehra et al.,

Journal of Chemical Health Risks

www.jchr.org

JCHR (2026) 16(2), 2743 - 2754

2022). These compounds exhibit inherent potential of antioxidant action through the scavenging of ROS and regulation of endogenous antioxidant enzyme systems, but their clinical implementation is limited by pharmacokinetic factors (Nehra et al., 2022).

Nanotechnology has become an innovative platform on which the therapeutic efficiency of plant-based antioxidants is increased by creating nano-sized delivery platforms. (Dinesh et al., 2025; Dinesh et al 2025) The metal-oxide nanoparticles and specifically the iron-oxide nanoparticles (FeNPs) have special interests that have arisen because of their biocompatibility, biodegradability, superparamagnetism and the inherent catalytic properties (Elahi & Rizwan, 2021; Dinesh et al., 2025). Traditional synthetic synthesis methods of FeNPs usually require the use of harsh chemical reducing agents (sodium borohydride, hydrazine), toxic solvents, and harsh reaction conditions, posing a risk to the environment and biocompatibility (Ajinkya et al., 2020). Green synthesis approaches, in contrast, utilize biologically available reducing agents (in particular, plant phytochemicals) to assist in nanoparticle formation at mild and ambient temperatures and confer a bioactive corona on top of the surface, which improves therapeutic activity (Ajinkya et al., 2020). Importantly, this procedure generates nanoparticles with grafted phytochemicals, which do not lose their bioactivity, and a multifunctional nanomaterial is obtained, in which the inorganic core and organic corona participate synergistically in the overall therapeutic effect (Ahmad et al., 2022). The iron-oxide core may be engaged in Fenton-like reactions, which may result in the formation of ROS under specific conditions; in other cases, such nanoparticles have ROS-scavenging properties in case they are surface-modified with antioxidant phytochemicals (Ge et al., 2022). Phytochemical corona provides initial radical neutralization through electron donation, and the ratio of surface area to volume of nanoparticles increases its accessibility to radical species (Liu et al., 2021; Akhtar et al., 2025). In addition, the nano-scale size also enables cellular internalisation which may carry antioxidants to intracellular location where oxidative stress is generated. Surface-bound phenolics metal chelate prevents transition-metal-catalyzed ROS production, and the nanoparticle scaffold could stabilize labile phytochemicals to oxidative degradation, increasing their functional lifetime (Liu et al., 2021).

Although preliminary studies are promising, there is lack of systematic comparative research studies on evaluation of the antioxidant performance of phytochemical-synthesized nanoparticles against plant extract as well as the standard antioxidants. Moreover, the precise role of the Capparis decidua phytochemicals in antioxidant activity of nanoparticles has not been well-defined to date. The interpretation of these synergistic interactions cannot be achieved without physicochemical characterisation of the synthesised nanomaterials in detail and quantitative evaluation of the synthesised nanomaterials in various complementary antioxidant assays that characterise different mechanistic pathways. The current study deals with the green preparation of FeNPs in Capparis decidua aqueous extract and the relative evaluation of their antioxidative ability.

2. Materials and Methods

2.1 Chemicals and Reagents

Ferric chloride hexahydrate ($FeCl_3 \cdot 6H_2O$, ≥ 99% purity) was procured from Merck (Darmstadt, Germany). 2,2-diphenyl-1-picrylhydrazyl (DPPH), 2,2'-azino-bis(3-ethylbenzothiazoline-6-sulfonic acid) diammonium salt (ABTS), and potassium persulfate were obtained from Sigma-Aldrich (St. Louis, MO, USA). Sodium nitroprusside dihydrate, sulfanilamide and N-(1-naphthyl)ethylenediamine dihydrochloride, and ascorbic acid (analytical grade) were purchased from HiMedia Laboratories (Mumbai, India). High-performance liquid chromatography (HPLC)-grade methanol, ethanol, and orthophosphoric acid were acquired from Merck. Ultrapure water (18.2 MΩ·cm resistivity) generated by a Milli-Q water purification system was employed throughout experimental procedures.

2.2 Plant Material Collection

Healthy, uninfected vegetative sections of Capparis decidua (Forsk.). Edgew. were collected in September 2023 on wild populations of arid areas. Morphological characteristics were used to do botanical authentication through the comparison with authenticated herbarium samples. The collected plant material was washed with tap water followed by ultrapure water to remove surface contaminants. The washed material was shade dried (preserving photosensitive bioactive compounds) in ambient temperature (22-25°C) for 10-15 days until constant weight was obtained. The dried material was ground to a fine powder (40-mesh sieve) in a mechanical grinder and the powder was put in amber glass vessels in

Journal of Chemical Health Risks
www.jchr.org
JCHR (2026) 16(2), 2743 - 2754

4 ℃ under desiccation conditions to maintain phytochemical integrity.

2.3 Preparation of Aqueous Plant Extract

A 1:10 w/v suspension of the dried powder was made in ultrapure water. The suspension was homogenized at 10000 rpm in a lab homogenizer for 5 minutes to disperse the suspension and release phytochemicals. The homogenate was subsequently placed in a temperature-regulated water bath and allowed to incubate at 60 ℃ with periodic stirring after every 30 min to assist extraction of heat-stable polyphenolic compounds without damaging fragile bioactives. The mixture was then cooled to room temperature and filtered through Whatman No. 1 filter paper and 0.45µm membrane filter convincingly to eliminate any particulate matter and cells debris. The resulting clear filtrate was directly used into the synthesis of nanoparticles.

2.4 Green Synthesis of Iron Oxide Nanoparticles

FeNPs were produced through a one-step green reduction process using the aqueous extract of Capparis decidua as a reducing as well as stabilising agent. About 100mL of the newly prepared extract was put in a 500mL glass beaker and heated to 60℃ with continuous magnetic stirring at 300rpm. Then, 100mL of a 0.1M ferric chloride hexahydrate solution was added dropwise at a rate of around 2mL/min with constant stirring. The extract-metal precursor molar ratio was maintained at 1:1 (v/v). The reaction mixture after the introduction of the ferric chloride initially exhibited a yellowish-brown colour, which gradually changed to dark brown and later to black in 2-3h, thus confirming the reduction of the Fe^{3+} in the reaction mixture and subsequent formation of iron oxide nanoparticles. During the synthesis, the temperature of the reaction was maintained at 60℃. The mixture was then left to cool to ambient temperature. Synthesized nanoparticles were separated through centrifugation at 10000 rpm for 15 minutes. The resulting precipitate was washed repeatedly (3-4 times) in ultrapure water and absolute ethanol to eliminate the unreacted ferric ions and other plant metabolites and soluble impurities. The pellet of the purified nanoparticle was resuspended in a low amount of ultrapure water and transferred to pre-weighed glass Petri dishes, then dried in a hot-air oven, 60 ℃ overnight until a stable weight was obtained. FeNPs were dried and then crushed to fine powder in a mortar and placed in sealed amber vials and kept under conditions of 4 ℃ in a desiccator.

2.6 Physicochemical Characterization

2.6.1 UV-Visible Spectroscopy

The equilibrium and stability of FeNPs were firstly determined with the help of UV-Vis absorption spectroscopy. Analysis of the nanoparticles was done by a Shimadzu UV 1800 double beam spectrophotometer in the wavelength range of 200-700nm with a resolution of 1nm using ultra-pure water as the blank. Before measuring the sample, baseline correction was done. Surface plasmon resonance (SPR) bands characteristic of iron oxide nanoparticles were identified from the absorption spectra.

2.6.2 Fourier Transform Infrared Spectroscopy

FTIR spectroscopy was used to identify functional groups that cause the reduction and stabilization of the nanoparticles. The KBr pellet method was used to prepare dried samples of purified FeNPs, where about 2-3mg of sample was thoroughly mixed with 200mg of spectroscopic-grade potassium bromide powder and pressed under hydraulic pressure (10tons) into clear discs. The infrared spectra were obtained using a PerkinElmer Spectrum Two FTIR spectrometer in transmittance mode on a mid-infrared range of 4000 to 4000cm-1 with a resolution of 4-1cm and 32 cumulative scans per sample. The pure KBr pellets were used to collect background spectra. Peak assignments were done by comparing observed wavenumbers with the literature of characteristic functional-group vibrations.

2.6.3 Dynamic Light Scattering and Zeta Potential Analysis

Dynamic light scattering (DLS) and zeta potential measurements were used to estimate the hydrodynamic particle size distribution and surface charge characteristics using a Malvern Zetasizer Nano-ZS instrument fitted with a He-Ne laser at 633nm and 173° backscatter detection optics. The FeNPs were dispersed into ultrapure water at a concentration of 0.1mg/mL and sonicated to remove any clumps of particles that could be present in the solution and then transferred to polystyrene cuvettes. Intensity-weighted size distributions were used to compute the Z-average hydrodynamic diameter and polydispersity index (PDI) by using algorithms based on Stokes-Einstein-equations. To measure the zeta potential, electrophoretic mobility of dilute suspensions of nanoparticles was measured by laser Doppler velocimetry by injecting dilute suspensions into folded capillary cells and zeta potential was calculated using the

Journal of Chemical Health Risks
www.jchr.org
JCHR (2026) 16(2), 2743 - 2754

Smoluchowski approximation. Each measurement was done in triplicate at 25℃.

2.7 In Vitro Antioxidant Activity Assays

2.7.1 DPPH Radical Scavenging Assay

The free-radical scavenging ability against 2,2-diphenyl-1-picrylhydrazyl (DPPH) was measured as described by Gulcin & Alwasel (2023). A stock solution of DPPH (0.1mM) was made in absolute methanol. FeNP samples were diluted to 20, 40, 60, 80, and 100 µg/mL) in methanol. To each concentration, 100 µL of the sample was mixed with 3.0ʿL of the DPPH solution in a disposable cuvette. At the same concentration levels, Ascorbic acid was used as a positive control, the negative control was the methanol and the DPPH solution. The mixtures of reaction were vortexed, and left to react in the dark at 25°C for 30 min to allow the radical-sample interaction to reach steady state. Absorbance was measured at 517nm with a methanol blank using UV-VIS spectrophotometer. The IC50 values were calculated by plotting the percent inhibition vs. sample concentration.

2.7.2 ABTS Radical Cation Scavenging Assay

The ABTS (2,2'-azino-bis(3-ethylbenzothiazoline-6-sulfonic acid)) radical-cation decolorisation test was performed according to the protocol as described by Thongsuk and Sameenoi (2022). ABTS radical cation was prepared by combining an equal portion of a 7mM ABTS diammonium salt solution with a 2.45mM potassium persulfate solution and letting the mixture stand in the dark at room temperature 12-16 h before use. The resulting ABTS+ stock solution that exhibited a typical blue-green colour was diluted with phosphate-buffered saline (pH 7.4) to an absorbance of 0.70 ± 0.02 at 734nm, thus forming the working reagent. In PBS, test samples (20-100µg/mL FeNP) were made. At each concentration, 100µl sample was added to 3ml of the ABTS+ working solution, vortexed, and left to incubate at room temperature at exactly 6 min in darkness. Absorbance was read at 734nm against PBS as blank. Ascorbic acid was the positive control. Dose response curves were then computed to give IC50

2.7.3 Nitric Oxide Radical Scavenging Assay

Nitric oxide (NO) radical scavenging activity was measured using sodium nitroprusside as an NO donor (Balkrishna et al., 2021). Sodium nitroprusside releases nitric oxide spontaneously in aqueous solution at physiological pH, which is then reacted with oxygen to produce nitrite ions which are measured spectrophotometrically with the Griess reagent. Sodium nitroprusside solution (10mM) was prepared in phosphate-buffered saline (pH7.4). The test samples solutions (20-100µg/mL FeNP) were combined with the same amounts of sodium nitroprusside solution into test tubes and incubated for 150min under fluorescent light at 25℃, to enable the generation of NO. After incubation, 500 µL of the reaction mixture were withdrawn and 500µl of Griess reagent was. The mixture was left in the darkroom at room temperature for 30 min to develop the chromophore. The absorbance was recorded at 546nm against blank. Ascorbic acid was used as positive controls. The dose-response curves were used to derive IC50.

2.8 Statistical Analysis

The experiments were performed in triplicate and the results were given as mean ± standard deviation (SD). The statistical analysis was done through GraphPad Prism version 9.0. To determine the significant differences between treatment groups, one-way analysis of variance (ANOVA) and post-hoc multiple comparison test (Tukey) were used. The statistically significant differences were considered at $p < 0.05$.

3. Results

3.1 Characterization of Green-Synthesized Iron Oxide Nanoparticles

3.1.1 UV-Visible Spectroscopy Analysis

UV-Visible spectroscopy was performed to monitor the bioreduction of ferric ions to iron oxide nanoparticles (Figure 1). The nanoparticles presented typical absorption peaks at 242, 385, 422, and 477nm. Such absorption bands are typical of surface plasmon resonance in iron oxide nanoparticles and occur as a result of collective oscillations of electrons in the conduction band in reaction to incident electromagnetic radiation. The highest point of 242nm is related to the electronic transition of small iron oxide clusters, and the high point in the long wavelength (385-477nm) to the bigger and well-formed nanoparticles. The continuous nanoparticle nucleation and growth with a rather homogeneous size distribution is evidenced by the increase in the intensity of the absorption without an apparent peak broadening or wavelength change over time. Lack of red shifts with aggregation implies good stabilization by phytochemical capping agents.

Journal of Chemical Health Risks

www.jchr.org

JCHR (2026) 16(2), 2743 - 2754

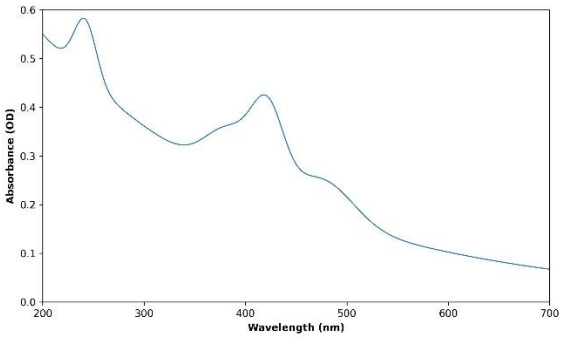

Figure 1. UV-Vis absorption spectra of *Capparis decidua*-FeNP's.

3.1.2 FTIR Spectroscopic Analysis

The FTIR spectrum of Capparis mediated-FeNPs showed multiple absorption bands, which proves the presence of different phytoconstituents involved in the reduction and stabilization of nanoparticles. Characteristic peaks of the high-frequency region (3842-3552 cm^{-1}) are associated with O-H stretching frequencies of hydroxyl groups, and denotes the presence of phenolic and alcoholic compounds as reducing agents. The additional peaks in region 3403-3262 cm^{-1} indicate the presence of hydrogen-bonded proteins or alkaloids as stabilizers. The absorptions bands in region 3098-2921 cm^{-1} indicate the C-H bonding of aliphatic and aromatic hydrocarbons, while the bands in 2837-2775 cm^{-1} may be due to aldehydic C-H bonds. Distinct peaks at 2502–2081 cm^{-1} are attributed to triple-bond stretching (C≡C/C≡N) which are characteristic of nitrile or alkyne groups. The 1817-1643 cm-1 absorptions are typical of C=O vibrations in esters, ketones, and amides, indicating the presence of biomolecules with carbonyl in the capping layer. The signal on 1541-1450 cm^{-1} is an indicator of N-H curvature and aromatic C=C, and the signal at 1387 cm^{-1} is a symmetric stretching of carboxylates. High peaks at 1189-999 cm^{-1} region indicate that there is C–O stretching of alcohols, ethers and polysaccharides establishing the presence of carbohydrates. Last but not least, Fe–O vibrations in the low frequency band of 734-664cm^{-1} is a measure of successful nanoparticle formation. The FTIR profile shows that hydroxyl, carbonyl, amide, and carboxylate groups of Capparis decidua phytochemicals were actively involved in Fe^{3+} reduction and provided stability to the FeNPs with the help of surface functionalisation.

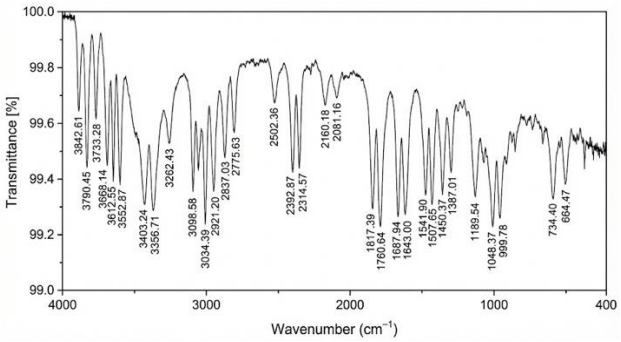

Figure 2. FTIR spectra of *Capparis decidua*-FeNP's.

3.1.3 Particle Size Distribution and Surface Charge

The intensity-weighted hydrodynamic size distribution of FeNPs in aqueous suspension was determined by the dynamic light scattering analysis (Figure 3A). The Z-average hydro dynamic diameter measured was 88.5nm with polydispersity index (PDI) of 0.46 which implies a fairly monodispersive particle population. The measurements of Zeta potential gave a result of -28.3 mV (Figure 3B) which is a moderate colloidal stability. The adverse surface charge maybe due to deprotonated carboxyl acid and phenolic hydroxyl groups of surface-adsorbed biomolecules (gallic acid, chlorogenic acid, quercetin) at neutral pH. DLVO (Derjaguin–Landau, Verwey, Overbeek) theory tells us that zeta potentials at the range of ±20 to ±30 0 mV give moderate aggregation stability and that above ±30mV zeta potential is excellent. The -28.3mV was an indication that electrostatic stabilization exists, but again, steric stabilization using large phytochemical molecules is also a factor that helps to avoid the agglomeration of particles. The absence of visible precipitation or colour change in stored nanoparticle suspensions post 10 days also determined colloidal stability.

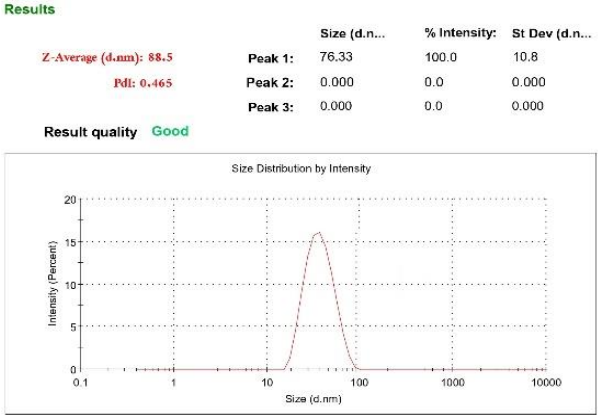

A

Journal of Chemical Health Risks

www.jchr.org

JCHR (2026) 16(2), 2743 - 2754

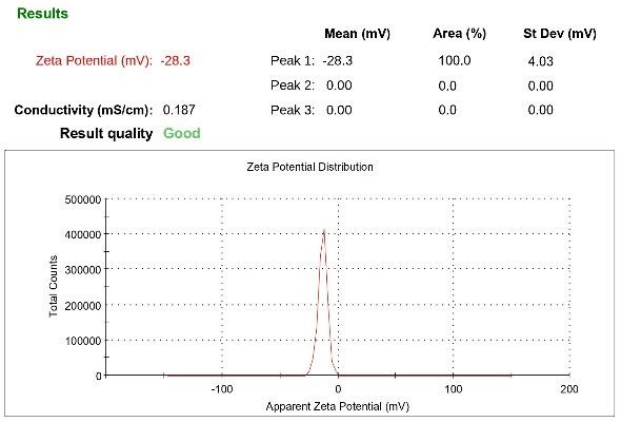

B

Figure 3. A) ZETA size, B) ZETA potential of *Capparis decidua*-FeNP's.

3.2 Antioxidant Activity Evaluation

3.2.1 DPPH Radical Scavenging Activity

The DPPH radical scavenging assay is a method to assess the antioxidant capacity of the substances on the basis of reducing the stable DPPH• radical (purple, λ_{max} 517 nm) to DPPH -H (yellow, non-absorbing) with the aid of hydrogen atom or electron transfer of antioxidants. Table-1 showed the dose-dependent DPPH radical scavenging of the extract of Capparis decidua and iron oxide nanoparticles (FeNPs). In the case of FeNPs, the percentage of scavenging increased from 15.05 ± 0.71% at 20 µg/mL to 74.44 ± 1.17% at 100 µg/mL, showing strong correlation with concentration (R2= 0.987). IC50 of FeNPs was calculated as 47.82 ± 1.86 µg/mL. Comparatively, the Ascorbic acid standard had a slightly better quality in terms of activity with IC50 = 43.25 ± 1.52 µg/mL, compared with the plant extract alone with IC50 = 66.45 ± 1.41 µg/mL significantly higher than the FeNPs ($p< 0.001$).

Table 1: Percent Radical Scavenging Activity Against DPPH

Concentration (µg/mL)	Ascorbic Acid (Mean ± SD)	Plant Extract (Mean ± SD)	FeNPs (Mean ± SD)
20	19.15 ± 0.84	12.84 ± 0.92	15.05 ± 0.71
40	36.38 ± 2.08	28.61 ± 1.76	34.27 ± 2.43
60	63.99 ± 1.84	45.73 ± 2.11	51.00 ± 1.87
80	76.24 ± 0.66	58.94 ± 1.39	63.81 ± 0.56
100	87.50 ± 1.17	70.26 ± 1.88	74.44 ± 1.17

The improved DPPH scavenging of FeNPs in comparison to the plant extract is a sign of synergy effects that occur due to the interaction between the phytochemicals and the nanoparticle. The 1.43-fold difference in the values of IC5O (from 66.45 to 47.82 µg/mL) indicates that the nanoparticle incorporation enhances the radical scavenging ability of the phytochemicals due to the multiplicity of the effects, namely: the larger the surface area, the greater the accessibility to DPPH radicals, the catalytic activity of the iron oxide core encourages the electron transfer and the stabilization of reactive phenolic radicals formed, after hydrogen donor (OH) addition, The fact that it is almost identical to ascorbic acid, a highly proven antioxidant, highlights the high free-radical scavenging ability of the green-synthesized nanomaterial.

3.2.2 ABTS Radical Cation Scavenging Activity

The $ABTS^{\bullet+}$ radical cation decolorization assay is used to complement mechanistic data with the fact that ABTS accepts both electrons and hydrogen atoms and is both soluble in water and organic solvents, so the hydrophilic and lipophilic antioxidants can be assessed. The concentration-dependent $ABTS^{\bullet+}$ scavenging of green-synthesized FeNPs ranged 8.24 ± 1.33% at 20 µg/mL to 70.57 ± 1.38% at 100 µg/mL (Table 2). The IC50 value was found to be 64.31 ± 0.97 µg/mL. The plant extract recorded IC50 = 81.76 ± 3.12 µg/mL, whereas ascorbic acid produced IC50 = 51.76 ± 2.02 µg/mL. The results of the statistical analysis supported the significant differences between FeNPs and the plant extract ($p<0.001$), whereby FeNPs were found to have a 1.36 fold higher potency.

Table 2: Percent Radical Scavenging Activity Against ABTS

Concentration (µg/mL)	Ascorbic Acid (Mean ± SD)	Plant Extract (Mean ± SD)	FeNPs (Mean ± SD)
20	18.62 ± 1.15	7.92 ± 1.21	8.24 ± 1.33
40	34.43 ± 0.76	19.48 ± 1.04	24.00 ± 0.80
60	57.71 ± 1.31	36.84 ± 1.89	56.81 ± 1.57
80	69.38 ± 1.58	48.97 ± 2.16	64.57 ± 2.29
100	84.86 ± 2.02	61.35 ± 1.74	70.57 ± 1.38

Journal of Chemical Health Risks

www.jchr.org

JCHR (2026) 16(2), 2743 - 2754

The results of the ABTS test are in line with those of the DPPH test, which supports the argument that nanoparticle-phytochemical conjugates have a higher antioxidant activity than that of phytochemicals. The observed slightly greater values of IC50 in the ABTS assay compared with DPPH of all test samples might be due to a variation in the radical stability, reaction kinetics or preferential mechanism of action. Catechol analogs of phenolic radical scavengers (found in large quantities in the plant, Capparis decidua) are especially efficient in ABTS because of their capacity to sequentially contribute several electrons. The synergetic improvement implies that the spatial positioning of phenolic hydroxyl groups is optimised in terms of radical neutralisation by the nanoparticle scaffold.

3.2.3 Nitric Oxide Radical Scavenging Activity

The nitric oxide is a physiologically and pathophysiologically relevant free radical species. In response to oxidative stress conditions, excessive production of NO is associated with the occurrence of peroxynitrite (ONOO-) which forms through the reaction of superoxide and, as a result, induces the nitration of proteins, lipid peroxidation, and DNA damage. FeNPs were tested for the NO scavenging ability by the use of sodium nitroprusside as an NO donor (Table 3). Findings have shown that it inhibits the accumulation of nitrite dose-dependently, with a scavenging percentage of 17.00 ± 1.23% at 20 µg/mL to 80.05 ± 0.80% at 100 µg/mL. This gave an IC50 of as 68.54 ± 0.79 µg/mL. Comparatively, plant extract indicated IC50 = 85.38 ± 2.86 µg/mL and ascorbic acid IC50 = 65.12 ± 0.57 µg/mL. FeNPs were 1.38 more potent as compared to the plant extract ($p<0.001$).

Table 3: Percent Radical Scavenging Activity Against NO

Concentration (µg/mL)	Ascorbic Acid (Mean ± SD)	Plant extract (Mean ± SD)	FeNPs (Mean ± SD)
20	19.32 ± 1.52	11.84 ± 1.36	17.00 ± 1.23
40	34.06 ± 1.67	22.67 ± 2.11	30.53 ± 2.76
60	44.25 ± 0.87	34.95 ± 1.78	43.82 ± 1.45
80	68.55 ± 0.66	46.88 ± 1.24	64.93 ± 0.52
100	84.20 ± 0.58	58.73 ± 1.69	80.05 ± 0.80

The strong NO radical scavenging properties of FeNPs have specific therapeutic potentials as disproportionate nitric oxide homeostasis is recognized to lead to inflammatory diseases, cardiovascular diseases and neurodegenerative diseases. The theory is that it is most probably the direct quenching of NO^* by the phenolic hydroxyl groups, possible chelation of the transition metals involved in catalyzing the oxidative damage through NO, and the blockage of the oxidation of NO to nitrite. The better performance of nanoparticle formulations over the extract implies that the high surface area and organization of presentations of antioxidant groups on the nanoparticle surfaces leads to more efficient NO interception.

3.2.4 Comparative Analysis and Synergy Assessment

The trend was observed in all the three complementary antioxidant assays: Ascorbic acid ≥ FeONPs > Plant Extract (Table 4). FeNPs had an averaged potency enhancement factor, which was 1.39-fold (significant in all assays) compared to the plant extract ($p <0.001$). To this end, the steady enhancement in mechanistically different assays, including DPPH (hydrogen atom transfer), ABTS (mixed mode), and NO (biological radical), is solid evidence of true synergistic antioxidant action and not results of assay-specific artifact.

Table 4. Comparative IC_{50} values (µg/mL) for antioxidant activities.

Sample	DPPH	ABTS	Nitric Oxide
Plant Extract	66.45 ± 1.41[a]	81.76 ± 3.12[a]	85.38 ± 2.86[a]
FeONPs	47.82 ± 1.86[b]	64.31 ± 0.97[b]	68.54 ± 0.79[b]
Ascorbic Acid	43.25 ± 1.52[b]	51.76 ± 2.02[c]	65.12 ± 0.57[c]

Values are mean ± SD (n=3). Different superscript letters within each column indicate significant differences ($p < 0.05$, Tukey's post-hoc test).

Synergistic interactions can be analyzed quantitatively by the combination index (CI) approach or by the fractional inhibitory concentration (FIC) index. A simplified synergy analysis was done that compared the hypothetical additive effect (when nanoparticle and phytochemicals would act independently) and the experimental effect. Assuming that it is purely additive, the IC50 of FeNPs would be similar to the IC50 of the plant extract, but at a fraction of the plant extract included. Nevertheless, the measured IC50 values were much lower than the expected additive ones, and the synergy indexes (theoretical IC 50/observed IC 50) of the

Journal of Chemical Health Risks
www.jchr.org
JCHR (2026) 16(2), 2743 - 2754

different assays were in the range of 1.35-1.45, which demonstrates that the interactions were super-additive or synergistic. This synergy is probably due to: (1) the improvement of phytochemical stability and bioavailability through nanoparticles; (2) a higher effective surface area through a larger radical-antioxidant collision frequency; (3) it may be intrinsic ROS-scavenging activity of the iron oxide core when surface-modified by antioxidants; and (4) multivalent presentation of antioxidant groups that allow radical to be neutralized cooperatively.

4. Discussion

This study presents the efficient eco-friendly production of iron-oxide nanoparticles using the aqueous extract of Capparis decidua as a reducing and stabilizing agent. The resulting nanomaterial has significantly increased antioxidant activity compared to the plant extract per se. The multifunctional antioxidant activity of the integration of phytochemicals with nanoparticles is supported by the observed synergistic improvement across three mechanistically different radical-scavenging assays. These findings are in agreement with the emerging evidence that the green-synthesized metal-oxide nanoparticles represent a convergence of sustainable nanotechnology and therapeutic efficacy, which propose unique benefits compared to traditional approaches to chemical synthesis. The typical UV-vis absorptions at the wavelengths of 242, 385, 422, and 477nm, prove the successful preparation of iron-oxide nanoparticles using surface plasmon resonance processes, consistent with previously reported FeNP synthesis Phoenix dactylifera and Thymus migricus extracts (Abdullah et al., 2020; Ashrafi-Saiedlou et al., 2025). The multiple absorption bands suggest that the material contains both phases; magnetite (Fe_3O_4) and maghemite (γ-Fe_2O_3), which are collectively responsible to the magnetic and catalytic characteristics of the material. The reduction mechanism mediated by phytochemicals is likely to be the electron donation of phenolic hydroxyl groups of the quercetin, kaempferol, gallic acid and chlorogenic acid that are available in Capparis decidua, which ultimately results in the conversion of Fe^{3+} to Fe^{2+} and the co-precipitation of mixed-valence iron-oxide phases. Similar mechanisms have been explained for Capparis species, including Capparis zeylanica and Capparis spinosa, which were successfully used to mediate gold and copper-oxide nanoparticle production, through polyphenolic compounds as primary reducing agents (Li & Li, 2025; Samari et al., 2019)

FTIR spectroscopic analysis showed the typical functional groups on the surfaces of the nanoparticles persisted, which meant that a phytochemical corona had been formed using a range of non-covalent interactions. (Dinesh et. al., 2025; Sutripto et al.; 2025) It is indicated by the retention of hydroxyl, carbonyl, carboxylate, and amide groups that bioactive compounds do not change their structure after nanoparticle decoration, thus maintaining their own antioxidant potential and at the same time, serving as a colloidal stabilizer. This effect is comparable to those obtained in the case of resveratrol-conjugated gold nanoparticles, where the higher the phytochemical corona density, the greater the therapeutic effect (Thipe et al., 2019; Neeraj et al.; 2025). Abraham et al. (2018) demonstrated the dynamically regulated corona formation of nanoparticles with phytochemical surface ligands, affecting nanoparticle-biological interface and ultimately bioavailability and therapeutic outcome. The moderate value of the zeta potential, -28.3mV, although reflecting reasonable colloidal stability, indicates that steric repulsion using large polyphenolic molecules plays an important role complementing electrostatic repulsion. Salavati et al. (2022) found that the zeta potential values above -30mV give optimum stability to the use of nanoparticles in therapeutic practice, and the moderate surface charge values may be compensated by the combined action of electrostatic and steric stabilization in the reference case of green-synthesized nanoparticles.

An increased antioxidant capacity of FeNPs compared to the plant extract in the DPPH, ABTS, and nitric-oxide radical-scavenging tests is the central finding of the current study. The average potency increase of 1.39 is a pointer of actual synergistic effect between the inorganic iron-oxide core and the organic phytochemical corona, and not mere additive effect. This synergy is likely to be caused by a number of complementary mechanisms. The nanoscale size (hydrodynamic diameter 88.5nm) has a tremendous surface area-volume ratio, making antioxidant functional groups in the nanoparticles highly exposed to radical species and increasing the frequency of collision between the radical and the neutralizing agent. The sequential electron transfer or hydrogen atom donation activities of the phenolic moieties presented on the surface of the nanoparticles may be enabled by the well-ordered arrangement of the phenolic compounds on the surface. Milenkovic et al. (2018) established that the

Journal of Chemical Health Risks

www.jchr.org

JCHR (2026) 16(2), 2743 - 2754

major Capparis decidua constituent gallic acid displays both hydrogen-atom transfer and proton-coupled electron transfer pathways, and the prevalence of the mechanism depends on radical species and microenvironment. The scaffold of nanoparticles can be optimally spatially oriented in phenolic groups so that each type of radical can optically occur in kinetically favorable reactions with the scaffold. It is possible that surface-bound polyphenols stabilize core of iron-oxide against Fenton-like reactions that might otherwise lead to the generation of hydroxyl radicals using hydrogen peroxide. Although, under specific conditions, bare iron-oxide nanoparticles may display pro-oxidant behavior, when coated with phytochemicals, they are transformed into antioxidant platforms, depending on metal chelation and electron donation (Abdelmonem & Albert, 2024; Abbas et al., 2025). Gulcin and Alwasel (2022) insisted that the presence of polyphenolic compounds stops oxidative damage of transition-metal catalyzed reactions through the chelation of Fe^{2+} and Cu^{2+}, preventing their ability to partake in the Fenton and Haber-Weiss reactions. This metal-chelating ability is built into the nanoparticle structure and performs a double role of stabilizing the iron core and at the same time capturing free transition metals in the biological settings. Nanoparticle formulation can help prevent oxidative degradation of labile phytochemicals to increase their operational lifespan versus free molecules, which are vulnerable to auto-oxidation. It is the nanoparticle matrix which forms a microenvironment that maintains an antioxidant activity over storage, and possibly over circulation in biological systems.The anti-oxidant capacity of FeNPs is especially relevant therapeutically because of their better performance on nitric-oxide scavenging. Imbalanced nitric -oxide homeostasis is implicated in inflammatory conditions, cardiovascular pathological conditions, and neurodegenerative disease by the formation of peroxynitrite and consequent biomolecular damage (Lakey -Beitia et al., 2021). The nanoscale delivery system has the potential to enable cellular uptake and intracellular compartmentalization and is able to act as an antioxidant at subcellular sites of oxidative stress such as mitochondria, endoplasmic reticulum and nucleus (Hood et al., 2014; Morshedi Rad et al., 2021). This is a significant benefit compared to free phytochemicals, which in many cases are poorly permeable to membrane and are poorly accumulated into the cell.

Even though the results in-vitro were promising, a number of shortcomings should be considered. Green synthesis has not yet been scalable because of variation in phytochemical composition on a seasonal basis, the possibility of batch-to-batch variability, and challenges in the standardization of the processes (Muslim et al., 2025; Đorđević et al., 2022). The regulatory frameworks of green-synthesized nanomedicines are in constant development, where extensive physicochemical characterization, stability verification, and toxicology evaluation should be performed before the clinical translation (Zheng et al., 2021). Moreover, in vitro antioxidant tests can offer a mechanistic understanding, but in vivo activity will rely on pharmacokinetic characteristics, such as half-life of circulation, biodistribution, efficiency of cellular uptake and immunogenicity. Yadav and Maurya (2021) have highlighted that therapeutic uses of metal-oxide nanoparticles must be thoroughly tested in oxidative stress models of illnesses in animals and safety profiles, as well as dose-response correlation, developed. Although the long-term outlook and biodegradability of iron-oxide nanoparticles is typically positive because of its integration into endogenous iron metabolism pathways (Fahmy et al., 2024), it needs to be confirmed in the context of the disease. Future investigations should focus on optimizing synthesis parameters to maximize antioxidant phytochemical loading, evaluating stability under physiological conditions, assessing cellular uptake mechanisms and intracellular distribution patterns, and conducting preclinical efficacy studies in animal models of oxidative stress-linked pathologies including neurodegenerative diseases, cardiovascular disorders, and diabetes. The integration of green chemistry principles with functional nanomaterial design, as demonstrated here with Capparis decidua-mediated synthesis, exemplifies sustainable nanotechnology approaches with potential to address global health challenges while minimizing environmental impact (Osman et al., 2024; Varma, 2016).

Conclusions

This study presents a viable and effective green synthesis of iron oxide nanoparticles utilizing Capparis decidua aqueous extract, whereby plant-derived phytochemicals operate simultaneously as reducing, stabilizing, and bio functionalizing agents. Comprehensive physicochemical evaluation indicated successful nanoparticle production with modest stability in colloids and a phytochemical-rich surface corona. The green-synthesized FeNPs demonstrated considerably improved antioxidant activity compared to the plant extract alone throughout DPPH,

Journal of Chemical Health Risks

www.jchr.org

JCHR (2026) 16(2), 2743 - 2754

ABTS, and nitric oxide scavenging assays, clearly exhibiting a synergistic interaction among the iron oxide core and surface-bound phytochemicals. This synergy is due to enhanced surface area, better radical accessibility, stability of active phenolic moieties, and cooperative electron/hydrogen transfer processes. In line with the concepts of green chemistry and sustainable nanotechnology, the results demonstrate the potential of phytochemical-mediated iron oxide nanoparticles as multifunctional, biocompatible antioxidant platforms, providing encouraging opportunities for therapeutic applications in disorders linked to oxidative stress.

Acknowledgements

The authors express their gratitude to Dr. Naresh for his help with the nanoparticle characterizations. One of the authors, Dinesh Kulhary, thanks Dr. Rajat Pandey and Anil Yadav for their insightful comments and encouraging words.

References

Abbas, R., Muzammil, S., Khurshid, M., & Hayat, S. (2025). Investigating the in vitro antibiofilm, antioxidant and photocatalytic potential of iron oxide nanoparticles biofabricated from Bauhinia variegata. *RSC advances*, *15*(54), 46009-46023.

Abdelmonem, M., Albert, E. L., Alhadad, M. A., & Abdullah, C. A. (2024). Plant-polyphenol-mediated synthesis of magnetic biocompatible iron oxide nanoparticles for diagnostic imaging and management of neurodegenerative diseases. *Precision Nanomedicine*, *7*(1), 1233-1251.

Abdullah, J. A. A., Eddine, L. S., Abderrhmane, B., Alonso-González, M., Guerrero, A., & Romero, A. (2020). Green synthesis and characterization of iron oxide nanoparticles by pheonix dactylifera leaf extract and evaluation of their antioxidant activity. *Sustainable Chemistry and Pharmacy*, *17*, 100280.

Abraham, A. N., Sharma, T. K., Bansal, V., & Shukla, R. (2018). Phytochemicals as dynamic surface ligands to control nanoparticle–protein interactions. *ACS omega*, *3*(2), 2220-2229.

Ahmad, K. S., Yaqoob, S., & Gul, M. M. (2022). Dynamic green synthesis of iron oxide and manganese oxide nanoparticles and their cogent antimicrobial, environmental and electrical applications. *Reviews in Inorganic Chemistry*, *42*(3), 239-263.

Ajinkya, N., Yu, X., Kaithal, P., Luo, H., Somani, P., & Ramakrishna, S. (2020). Magnetic iron oxide nanoparticle (IONP) synthesis to applications: present and future. *Materials*, *13*(20), 4644.

Al-Madhagi, H., & Masoud, A. (2024). Limitations and challenges of antioxidant therapy. *Phytotherapy Research*, *38*(12), 5549-5566.

Ashrafi-Saiedlou, S., Rasouli-Sadaghiani, M., & Fattahi, M. (2025). Green synthesis of iron oxide nanoparticles using Thymus migricus for multifunctional applications in antioxidant, antimicrobial, photocatalytic, and seed priming processes. *Heliyon*, *11*(5).

Ayan, A., Daniyal, A., & Rehan, A. (2025). Capparis decidua: Phytochemical and Pharmacological Review. *International Journal of Research in Pharmacy and Allied Science*, *4*(3), 36-42.

Balkrishna, A., Kumar, A., Arya, V., Rohela, A., Verma, R., Nepovimova, E., ... & Kuca, K. (2021). Phytoantioxidant functionalized nanoparticles: a green approach to combat nanoparticle-induced oxidative stress. *Oxidative medicine and cellular longevity*, *2021*(1), 3155962.

Bartsch, H., & Nair, J. (2006). Chronic inflammation and oxidative stress in the genesis and perpetuation of cancer: role of lipid peroxidation, DNA damage, and repair. *Langenbeck's Archives of Surgery*, *391*(5), 499-510.

Deshmukh, A. R., Gupta, A., & Kim, B. S. (2019). Ultrasound assisted green synthesis of silver and iron oxide nanoparticles using fenugreek seed extract and their enhanced antibacterial and antioxidant activities. *BioMed research international*, *2019*(1), 1714358.

Đorđević, S., Gonzalez, M. M., Conejos-Sánchez, I., Carreira, B., Pozzi, S., Acúrcio, R. C., ... & Vicent, M. J. (2022). Current hurdles to the translation of nanomedicines from bench to the clinic. *Drug delivery and translational research*, *12*(3), 500-525.

Eghbaliferiz, S., & Iranshahi, M. (2016). Prooxidant activity of polyphenols, flavonoids, anthocyanins and carotenoids: updated review of mechanisms and catalyzing metals. *Phytotherapy Research*, *30*(9), 1379-1391.

Elahi, N., & Rizwan, M. (2021). Progress and prospects of magnetic iron oxide nanoparticles in biomedical

applications: A review. *Artificial Organs*, *45*(11), 1272-1299.

Dinesh Kulhary and Neeraj Dhariwal, An Investigation into the Structure, Microhardness, Intermolecular Interactions, Electrical and Optical Properties in Lead-Free $(CH_3CH_2CH_2NH_3)_2[BiCl_5]$ Single Crystals for Optoelectronic Applications. Material Science and Engineering B: 321 (2025) 118552.

Fahmy, H. M., Shekewy, S., Elhusseiny, F. A., & Elmekawy, A. (2024). Enhanced biocompatibility by evaluating the cytotoxic and genotoxic effects of magnetic iron oxide nanoparticles and chitosan on Hepatocellular Carcinoma Cells (HCC). *Cell Biochemistry and Biophysics*, *82*(2), 1027-1042.

Ge, X., Cao, Z., & Chu, L. (2022). The antioxidant effect of the metal and metal-oxide nanoparticles. *Antioxidants*, *11*(4), 791.

Gulcin, İ., & Alwasel, S. H. (2022). Metal ions, metal chelators and metal chelating assay as antioxidant method. *Processes*, *10*(1), 132.

Gulcin, İ., & Alwasel, S. H. (2023). DPPH radical scavenging assay. *Processes*, *11*(8), 2248.

Hood, E. D., Chorny, M., Greineder, C. F., Alferiev, I. S., Levy, R. J., & Muzykantov, V. R. (2014). Endothelial targeting of nanocarriers loaded with antioxidant enzymes for protection against vascular oxidative stress and inflammation. *Biomaterials*, *35*(11), 3708-3715.

Jomova, K., Raptova, R., Alomar, S. Y., Alwasel, S. H., Nepovimova, E., Kuca, K., & Valko, M. (2023). Reactive oxygen species, toxicity, oxidative stress, and antioxidants: chronic diseases and aging. *Archives of toxicology*, *97*(10), 2499-2574.

Kovacic, P., Somanathan, R., & Z Abadjian, M. C. (2015). Natural monophenols as therapeutics, antioxidants and toxins; electron transfer, radicals and oxidative stress. *The Natural Products Journal*, *5*(3), 142-151.

Lakey-Beitia, J., Burillo, A. M., La Penna, G., Hegde, M. L., & Rao, K. S. (2021). Polyphenols as potential metal chelation compounds against Alzheimer's disease. *Journal of Alzheimer's Disease*, *82*(s1), S335-S357.

Li, Z., & Li, S. (2025). Biogenic synthesis of gold nanoparticles using Capparis zeylanica extract and their oxidative and cytotoxic effects on colorectal cancer cells. *Journal of Nanostructure in Chemistry*, *15*(3).

Kulhary D., Majumder S., Erum Gul Naz, Yogendra Singh, Sunita Shalabh Pachori, Sainath Narayan Bhavsar, Manish R. Bhise, Bismuth-based organic-inorganic hybrid perovskite $[C_{10}H_{16}N]_2BiCl_5$ as a novel visible-light active photocatalyst for the degradation of rhodamine B dye and ciprofloxacin antibiotic, Materials Science in Semiconductor Processing, 204 (2026) 110317.

Majumder S., Swapnil S. Karade, Raman Kumar, Raja Venkatesan, Dinesh, Sarah A. Alshehri, Hieu Minh Nguyen, Ki Hyeon Kim, Unlocking the potential of Fe_2TiO_5 nanoparticles: A promising pseudocapacitive material for next-generation supercapacitors, Materials Science in Semiconductor Processing, 202, 2026, 110194.

Liu, J., Ma, L., Zhang, G., Chen, Y., & Wang, Z. (2021). Recent progress of surface modified nanomaterials for scavenging reactive oxygen species in organism. *Bioconjugate Chemistry*, *32*(11), 2269-2289.

Akhtar, V.; Kulhary, D. Physico-Chemical Characterization and Environmental Implications of Jarosite Waste from Zinc Hydrometallurgical Processing. *ajc* **2025**, *37*, 1995-2001.

Milenković, D., Đorović, J., Petrović, V., Avdović, E., & Marković, Z. (2018). Hydrogen atom transfer versus proton coupled electron transfer mechanism of gallic acid with different peroxy radicals. *Reaction Kinetics, Mechanisms and Catalysis*, *123*(1), 215-230.

Morshedi Rad, D., Alsadat Rad, M., Razavi Bazaz, S., Kashaninejad, N., Jin, D., & Ebrahimi Warkiani, M. (2021). A comprehensive review on intracellular delivery. *Advanced Materials*, *33*(13), 2005363.

Muslim, M. R. F., Chabib, L., Suryaningsih, B. E., Suciati, T., & Rusdiana, T. (2025). Green-synthesized silver nanoparticle hydrogels for biofilm-infected wounds: Bridging sustainability and clinical translation. *Frontiers in Pharmacology*, *16*, 1694144.

Nehra, S., Gothwal, R. K., Varshney, A. K., Meena, P., Ghosh, P., & Trivedi, P. C. (2022). Bioactives and Pharmacology of *Capparis decidua* (Forssk.) Edgew.(Syn.: *Capparis aphylla Roth*). In *Bioactives and Pharmacology of Medicinal Plants* (pp. 207-220). Apple Academic Press.

Journal of Chemical Health Risks

www.jchr.org

JCHR (2026) 16(2), 2743 - 2754

Dinesh, Temperature-Responsive Opto-Electrical Characteristics combined with Reversible Thermochromism in copper chloride Hybrid Perovskite for smart window applications, Ceramics International: 51 (17), 2025, 23021–23032.

Dinesh and Arun Sharma, Photoluminescent behaviour combined with electrical and optical properties in manganese (II) halide perovskite for photoluminescent rewritable printing applications, Ceramics International: 51 (20) 2025, 31359-31369.

Osman, A. I., Zhang, Y., Farghali, M., Rashwan, A. K., Eltaweil, A. S., Abd El-Monaem, E. M., ... & Yap, P. S. (2024). Synthesis of green nanoparticles for energy, biomedical, environmental, agricultural, and food applications: A review. *Environmental Chemistry Letters*, *22*(2), 841-887.

Pal, S., Prasad, R. S., Prasad, S. K., Goyal, R. K., & Dhobi, M. (2021). An Updated Overview of Ethnomedicinal Uses, Phytochemical and Various Pharmacological Evaluations on the Plant *Capparis decidua* (Forssk.) Edgew. *Current Traditional Medicine*, *7*(2), 189-202.

Salavati, M. S., Amini, S. M., Nooshadokht, M., Shahabi, A., Sharifi, F., Afgar, A., ... & Mirzaei-Parsa, M. J. (2022). Enhanced colloidal stability of silver nanoparticles by green synthesis approach: characterization and anti-leishmaniasis activity. *Nano*, *17*(07), 2250052.

Samari, F., Baluchi, L., Salehipoor, H., & Yousefinejad, S. (2019). Controllable phyto-synthesis of cupric oxide nanoparticles by aqueous extract of Capparis spinosa (caper) leaves and application in iron sensing. *Microchemical Journal*, *150*, 104158.

Thipe, V. C., Panjtan Amiri, K., Bloebaum, P., Raphael Karikachery, A., Khoobchandani, M., Katti, K. K., ... & Katti, K. V. (2019). Development of resveratrol-conjugated gold nanoparticles: Interrelationship of increased resveratrol corona on anti-tumor efficacy against breast, pancreatic and prostate cancers. *International journal of nanomedicine*, 4413-4428.

Dhariwal N., Preety Yadav, Dinesh, Somdatta Singh, Amit Sanger, Ramesh Chandra, O.P. Thakur, Vinod Kumar, Tailored 2D Bi_2WO6-rGO hybrid composites for advanced flexible and wearable supercapacitor devices, Inorganic Chemistry Communications, 182, 2025, 115398.

Thongsuk, P., & Sameenoi, Y. (2022). Colorimetric determination of radical scavenging activity of antioxidants using Fe3O4 magnetic nanoparticles. *Arabian Journal of Chemistry*, *15*(1), 103475.

Varma, R. S. (2016). Greener and sustainable trends in synthesis of organics and nanomaterials. *ACS Sustainable Chemistry & Engineering*, *4*(11), 5866–5878.

Yadav, S., & Maurya, P. K. (2021). Biomedical applications of metal oxide nanoparticles in aging and age-associated diseases. *3 Biotech*, *11*(7), 338.

Zheng, C., Li, M., & Ding, J. (2021). Challenges and opportunities of nanomedicines in clinical translation. *Bio Integration*, *2*(2), 57